ELSEVIER

Polymer 42 (2001) 7033–7047

polymer

www.elsevier.nl/locate/polymer

Epitaxy of isotactic poly(1-butene): new substrates, impact and attempt at recognition of helix orientation in form I′ by AFM

C. Mathieu[a], W. Stocker[b], A. Thierry[a], J.C. Wittmann[a], B. Lotz[a,*]

[a]*Institut Charles Sadron, CNRS–ULP, 6, rue Boussingaults, 67083 Strasbourg, France*
[b]*Institut für Physik, Humboldt Universität zu Berlin, Invalidenstrasse 110, D-10115 Berlin, Germany*

Received 31 August 2000; received in revised form 2 February 2001; accepted 2 March 2001

Abstract

Epitaxial crystallization of isotactic poly(1-butene) (iPBu) is performed on different substrates, which help expand the range of interactive substrates used in a previous study. All three crystal forms of iPBu1, which rest on different helix and unit-cell geometries and symmetries, have been produced by epitaxial crystallization. The different epitaxial interactions are discussed. Epitaxial crystallization of form I′ yields an exposed (110) contact plane. The films have true single crystal structure; they display electron diffraction patterns with sharp peaks, but also characteristic streaks due to the co-existence of up and down helices in the crystal structure (anticline helices). The streaks are modelled with a 'Diffraction faulted' program. Further, this same (110) contact face of Form I′ provides the potential to observe in direct space (i.e. by AFM) the up or down orientation of helices. Such a possibility would require differentiation by AFM of a methyl group from an ethyl group of the side chains. The AFM resolution reached in our investigation falls short of doing so, but the problematics could be adapted to other, more suitable polymers.

Keywords: Isotactic Poly(1-Butene); Epitaxy; Atomic force microscopy

1. Introduction

Isotactic poly(1-Butene) (iPBu1) can exist in three different crystal phases which differ by the chain conformation and, as a result, the unit-cell geometry and symmetry. Form II is produced spontaneously on bulk crystallization; it has an 11_3 helix geometry and a tetragonal unit-cell. Form I is isostructural with Form I′; they have a 3_1 helix geometry and a trigonal unit-cell; Form I is obtained by spontaneous crystal–crystal transformation of Form II on ageing, whereas Form I′ is produced by direct crystallization. Form III, produced only from dilute solution, has a 4_1 helix conformation and an orthorhombic cell geometry [1].

Crystallization induced by epitaxy on specific substrates is a very powerful means to induce the various polymorphic forms of polymers [2]. When applied to iPBu1, epitaxial crystallization has made it possible to induce all three forms (II, I′ and III) from the melt [3,4]. A major advantage of epitaxial crystallization is that it yields highly oriented or even single crystal orientations. This holds for crystal modifications which are unstable to mechanical shear, and cannot be oriented by other means. As an illustration, the crystal structure of Form III of iPBu1 could be reanalyzed on the basis of extensive electron diffraction data gathered from single crystals and epitaxially crystallized films [5].

In the present paper, we explore further various aspects of the epitaxial crystallization of iPBu1. We analyze the epitaxial relationships of yet different substrates and their versatility towards the crystal phases of iPBu1. We amend and complete the epitaxy rules of helical polymers on crystalline substrates, illustrated so far mainly with isotactic polypropylene (iPP) [6,7]. iPBu1 provides indeed a second polymer for which the whole range of possible interactions are involved: chain axis repeat distance, interchain distance, distance between successive helical turns.

We also exploit the epitaxially crystallized films to analyze details of iPBu1 structure, and more specifically the relative helix sense in Form I or I′. As noted very early on by Natta and Corradini [8], up- and down-pointing helices of iPBu1 Form I are nearly isosteric, which makes it possible to substitute an up- by a down-pointing helix at any chain site (the two helices are defined as *anticline* rather than antiparallel, since conformational rather than chemical differences are at play; parallel helices are *isocline* or *syncline*). A structure based on isocline helices only has space group R3c; statistical half occupancy at each chain

* Corresponding author. Tel.: +33-03-88-41-40-46; fax: +33-03-88-41-40-99.
E-mail address: lotz@ics.u-strasbg.fr (B. Lotz).

0032-3861/01/$ - see front matter
PII: S0032-3861(01)00185-9

site of up- and down-pointing helices corresponds to space group symmetry R-3c. In these very thin films (≈10 nm), up-down chain orientation corresponds to a structural disorder, which generates streaks in the diffraction pattern [4]. These are analyzed with a modelization program.

Oriented films of Form I′ with their exposed (110) contact face provide also a material potentially suited to observe by atomic force microscopy (AFM) *the relative orientation of individual helical stems in direct space*. Such a visualization would be a further step in the 'direct' analysis of polymer crystal structures by AFM, following the observation of the pattern of methyl groups in the contact face of epitaxially crystallized iPP [9,10], the visualization of the frustrated crystal structure of the β phase of iPP [11] and the observation in direct space of the helical hands (right and left) in syndiotactic polypropylene (sPP) [12]. As will be shown, discrimination between up- and down-pointing iPBu1 helices would require being able to distinguish by AFM a methyl group from an ethyl group in the contact face. Although our images fall slightly short of doing so, it is of interest to illustrate the concepts, and describe the experimental procedures and technical challenges encountered in this endeavour, which may be transposed to other, similar but better adapted systems.

2. Materials and experimental procedures

Isotactic poly(1-butene) is a low molecular weight material purchased from Aldrich. The nucleating agents used during this work are 4-chlorobenzoic acid (4ClBzAc), 4-bromobenzoic acid (4BrBzAc), 3-fluorobenzoic acid (3FlBzAc) and a nucleating agent patented for the β phase of isotactic polypropylene by New Japan Chemical [13], dicyclohexylterephthalamide (DCHT) of formula:

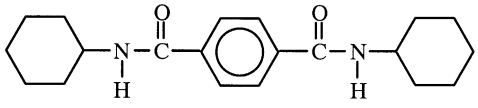

The experimental procedures are as described in several previous works and reviews [2–4]. It rests on the production of a thin polymer film (usually produced by evaporation from a ≈1% solution in *p*-xylene) on a glass cover slide and orientation by a low molecular weight crystalline substrate, either spread on the polymer film and co-melted, or produced as single crystals in a different crystallization experiment and deposited on the polymer film prior to melting and recrystallization of the latter. The crystalline substrate is redissolved, leaving a thin polymer film with the imprint of the substrate crystals, and with the contact face exposed. These films can be used as such for AFM investigations: the location of the zones of interest by optical microscopy is facilitated by the imprints left in the polymer films by the substrate crystals. For electron microscopy investigations, they are shadowed (if desired), backed with a carbon film, removed from the support glass cover with the help of a polyacrylic acid backing, and mounted on electron microscope grids.

Electron microscopy and diffraction are performed with a Philips CM12 microscope operated at 120 kV in the defocused electron diffraction mode and diffraction mode to limit electron beam damage to the iPBu1 film, which is very beam sensitive. AFM examination is performed with Digital Instruments Nanoscope II or III essentially under the same conditions as used in a previous investigation on the β phase of iPP: contact mode, A-type scan head, Si_3N_4 tips, microfabricated cantilever (triangular base, 200 μm) with a 0.06 N/m force constant. The imaging is performed in a liquid cell (2-propanol), and the areas of interest of the sample (indicated by the imprint of the substrate crystals in the polymer film) are prepositioned near the center with the help of an optical microscope. Scanning line frequencies are up to 54 Hz for high resolution work. An unfiltered deflection image is presented in this paper.

The crystal structures and diffraction patterns are generated with the appropriate modules of the Cerius 2 program (Molecular Simulations, Waltham, USA and Cambridge, UK) [14]. The streaks are generated with the 'Diffraction Faulted' module of the same program. It is based on a Fortran program written by Newsam and Treacy [15]. Four different crystal structures can be considered, which are packed according to different probabilities. Random shifts can be included. The program delivers either simulated electron or X-ray diffraction patterns, or intensity profiles on the various layer lines. Only the latter display mode is used in the present investigation.

3. Results and discussion

The present section is organized in two parts: first, the results of epitaxial crystallization of iPBu1 on different crystalline substrates is presented. This work extends and complements an earlier investigation on the same theme [3,4]. Next, the issue of helical sense in epitaxially crystallized films of form I′ is addressed, using two different approaches: analysis of the diffraction pattern, which provides a global approach of the disorder, and the more local approach made possible by AFM.

3.1. Polymorphism of iPBu1 induced by epitaxy

Epitaxial crystallization of iPBu has been shown in a previous investigation to induce the three crystal polymorphs, with their different helical conformations. Only a limited number of substrates had been tested, and the results were analyzed mainly in terms of lattice matching.

Epitaxy of form II was achieved on benzoic acid, which induces two chain orientations nearly at right angles to each other. Analysis of the epitaxy is complicated by the fact that two antichiral helices are present in the (100) contact face of the polymer, and further the helices

have a non-crystallographic symmetry: 11_3. These helices are 7.71 Å apart, which fits the distance between two interplanar (110) distances in benzoic acid (7.51 Å) [3].

Epitaxy of Form I′ is best understood [4]: this form is generated with substrates that display a linear grating with 6.3 Å periodicity. The (110) plane of the trigonal unit-cell is the contact plane. This plane exposes isochiral three-fold helices, with their 'flat' face (in *c* axis projection) exposed. The side chains of iPBu1 form a linear grating in this face, with a similar 6.3 Å periodicity, which is tilted to the chain axis, and actually parallel to the (102) planes of the crystal lattice. The epitaxy is 'chirality dependent': the tilt of the chain axis is different when right-handed helices or left-handed helices are exposed, and this chirality can be 'read' from the observed tilt.

Epitaxy of Form III was obtained only when using 2-Quinoxalinol as a substrate [3]. One chain orientation only was obtained, and the analysis of the epitaxy suggests a one dimensional correspondance between the chain axis repeat distance (7.56 Å) and a similar substrate periodicity. The contact plane is (110) of the orthorhombic unit-cell, which has a complex topography [5]: two (isochiral) 4_1 helices of iPBu1 with different azimuthal settings are exposed, which complicates the analysis of the interactions.

The above results and analyses are tested in the face of new investigations with different nucleating agents. We present first new results obtained with 4-chloro and bromobenzoic acid (already used in a previous investigation) which initiate forms II and I′, then turn to dicyclohexylterephthalamide (DCHT), before analyzing the epitaxies of iPBu1 on 3-fluorobenzoic acid, which is able to induce *all three crystal polymorphs of iPBu1*. This section is concluded with a summary of the structural rules for the epitaxial crystallization of helical polymers, based on present and prior results, obtained with e.g. isotactic polypropylene.

3.1.1. Epitaxies of iPBu1 on 4-chloro- and bromobenzoic acid: Forms I′ and II

4-Chloro- and bromobenzoic acids (4ClBzAc and 4BrBzAc, respectively) have been used in a previous investigation [3,4] and shown to induce the epitaxy of Forms II and I′ of iPBu1. However, what appears now as a rather artificial dichotomy between the two substrates was made according to the predominance of one form over the other. The newer results obtained with these substrates suggest that they have a very similar behavior, and that they are able to induce both forms.

The unit-cell parameters of 4-chlorobenzoic acid are: $a = 14.39$Å, $b = 6.23$ Å, $c = 3.86$ Å, $\alpha = 88.68°$, $\beta = 100.12°$, $\gamma = 93.31°$, space group $P2_1/a$ [16] and for 4-bromobenzoic acid: $a = 29.52$Å, $b = 6.15$ Å, $c = 3.98$ Å, $\alpha = \gamma = 90°$, $\beta = 1095.5°$, space group $P2_1/a$ [17]. In both cases, the contact plane is *bc* and the structural feature at play in the epitaxy is the rows of chlorine (or bromine) atoms ≈ 6.2 Å apart. Epitaxial crystallization of iPBu1 on 4Cl- or 4BrBzAc is vividly illustrated in the optical micrographs (phase contrast and crossed polars) displayed in Fig. 1. The middle figure shows the epitaxially crystallized thin film after dissolution of the substrate: two sets of edge-on lamellae are clearly visible. The chain orientations within these sets of lamellae are best determined by using crossed nicols: when the lamellae are rotated by either + or −24° in order to bring the chains within one or the other set of lamellae parallel to the

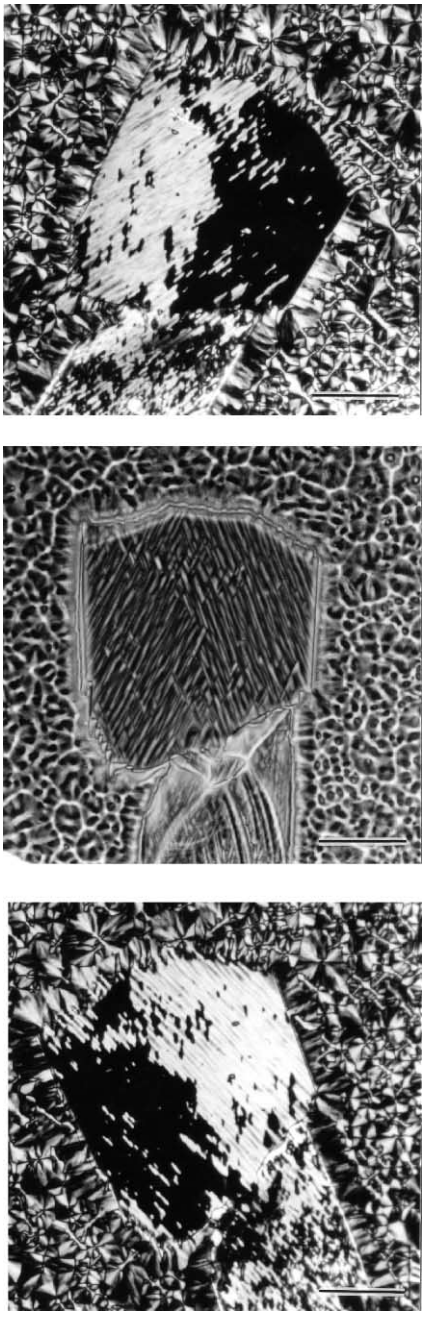

Fig. 1. Epitaxial crystallization of Form II on 4-chlorobenzoic acid crystals. Orientation of the edge-on lamellae grown on the substrate single crystal is best revealed by phase contrast optical microscopy (middle). Examination under crossed nicols of the film rotated by + and −24° brings one or the other population of lamellae in extinction (right and left). Scale bar: 50 μm.

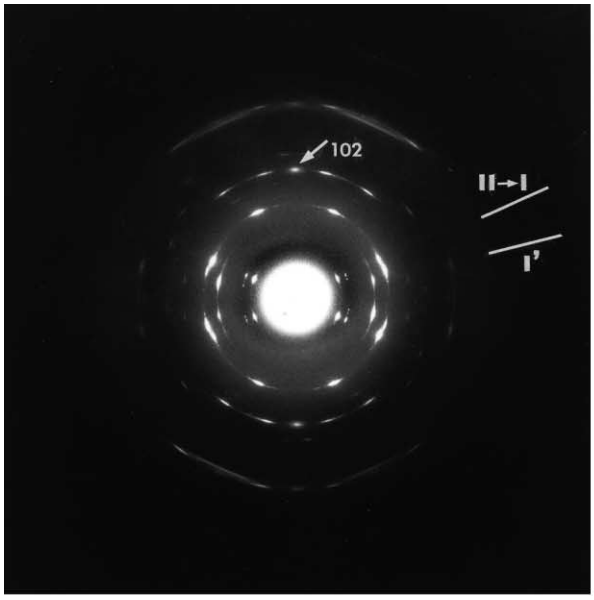

(a)

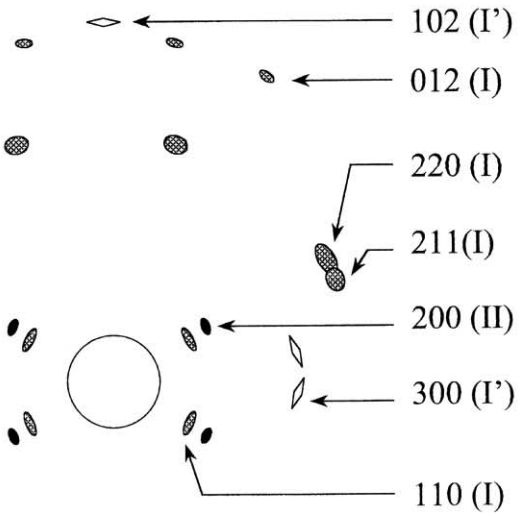

(b)

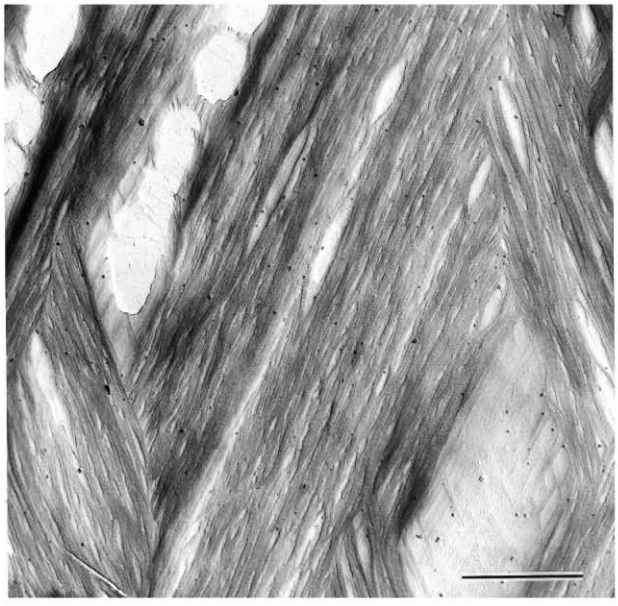

(c)

Fig. 2. (a) Selected area electron diffraction pattern of a film as shown in Fig. 1, with indication of the two equators (b) indexing of the pattern on the basis of Forms I′, II and I lattices (c) bright field electron micrograph of a similar area. The Form II structure is in the process of transformation into Form I. Scale bar: 2 μm.

polarizer or analyzer, the corresponding areas become extinct. A diffraction pattern and representative bright field corresponding to such films are displayed in Fig. 2. Analysis of these electron diffraction patterns reveals that there are not two, but rather four different chain orientations present in the film (two equators indicated in Fig. 2(a), indexing in Fig. 2(b)). The analysis is also complicated by the interference of a Form II → I crystal–crystal transformation [18–20]. It is therefore of interest to detail the structural information provided:

- The patterns indicate *four* different chain axis orientations, which are tilted at ±24° and ±12° relative to the *common bisector* of these orientations. Interestingly, the diffraction pattern is more legible than the bright field: indeed, the two chain orientations at ±12° of

Form I′ are obvious from diffraction evidence, but the corresponding lamellae are not easy to discern in the micrographs.

- All four orientations correspond to diffraction patterns of Form I and/or I′, as indicated by the organization of the diffraction spots on layer lines 1/6.5 Å apart
- The four patterns of Form I and/or I′ are not equivalent. Indeed:
  - the two inner patterns (corresponding to ±12° tilts) are *asymmetric* relative to their chain axis orientation. This is best illustrated by the single strong reflection on the second layer line (indexed as 102), or by the asymmetry of diffraction intensities on the fourth layer line (better visible later, cf. Fig. 6). As will be shown, these patterns correspond to epitaxial crystallization directly in Form I′. They are analyzed in better detail later, when examining the structural disorder of this form. We note for future reference that in these patterns, the spots on the 'equator' are indexed as 300: the contact plane is (110) of the trigonal unit-cell.
  - the two outer patterns (corresponding to ±24° tilts, cf. Fig. 2) are *symmetric* relative to their chain axis orientation, as indicated by the presence of *two* 102 reflections on the second layer line. These patterns correspond to Form I, and are actually the result of a crystal–crystal transformation: iPBu1, initially crystallized in Form II, has transformed into Form I; the transformation, which is spontaneous, is much faster under the electron beam [3]. The present patterns are taken near the end of the transformation, but traces of the initial Form II are still visible (cf. the equatorial reflections). The equatorial reflections of Form II are indexed as 200: the contact plane is of (100) type.

As a result of the above structural analysis, we recall for future reference that (i) epitaxial crystallization *directly* in form I′ yields *asymmetric patterns*, even if two orientations coexist and yield a symmetric but *composite* pattern, and that (ii) epitaxy initially in Form II yields, after II → I crystal–crystal transformation, *symmetric* patterns of Form I, which is isostructural to Form I′.

Before closing this section, a minor, but essential difference between Form I′ and Form I (ex-Form II) patterns must be pointed out and analyzed. On the 'equator' of the Form I′ pattern, only 300 spots (and its second order) are visible; on the 'equator' of Form I (ex Form II), 110 and 220 are most prominent, whereas 300 is weak. This difference results from the details of Form I′ and Form II epitaxies, and the constraints on Form II → I transformation [18–21]. As shown in Fig. 3(a), epitaxy of Form I′ involves the (110) contact plane, which means that the (300) planes are in diffracting position. As shown on the right side of Fig. 3(a), upon 'spontaneous' II → I crystal–crystal transformation, the (110) planes of the tetragonal Form II become (110) of the trigonal form I: this transformation process preserves the chirality of the helices upon transformation since in both forms, the layers are isochiral, with successive layers being antichiral. Given this structural constraint [19–21], the contact plane of form II should be (110) in order to yield, after transformation, an orientation of the Form I lattice similar to Form I′ (Fig. 3(a), right). The epitaxial contact plane is however $(100)_{II}$, which is further constrained by the support carbon film (Fig. 3(b)). As a result, the transformation takes place by shearing along $(100)_{II}$ rather than $(110)_{II}$, the parallelism of $(110)_{II}$ and $(110)_{I}$ is no longer preserved and the *hh* 0 planes of Form I are in diffraction position (Fig. 3(b)).

3.1.2. Epitaxy of iPBu1 on dicyclohexylterephthalamide: Forms II and III

Dicyclohexylterephthalamide (DCHT) is known as a nucleating agent specific for the β phase of isotactic polypropylene [11,13,22]. Its crystal structure is not yet determined (to our knowledge), but electron diffraction patterns suggest that in the contact plane it forms a rectangular array ≈6.7 Å by ≈5.2 Å (assuming an orthorhombic cell projection). It turns out that DCHT can also induce the crystallization of iPBu1, and more specifically of its Forms II and III.

The diffraction pattern and lamellar structure (revealed by gold decoration) of a composite film in which forms II and III coexist is shown in Fig. 4. The major difference with the

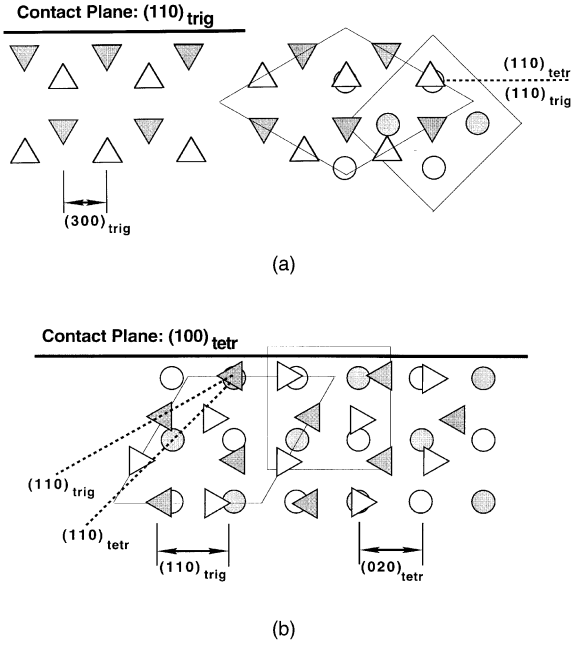

Fig. 3. (a) Orientation of Form I′ unit-cell in the epitaxially crystallized thin film: the (300) planes (or similar planes) are in diffracting conditions. As a result of the chirality constraints of the Form II to I transformation, a similar orientation of Form I would be produced if the Form II contact plane were (110) (right side of the figure). Three fold helices of the trigonal unit-cell are shown as triangles, 11_3 helices of the tetragonal cell as circles; opposite helix chiralities are indicated as shaded and unshaded. (b) Orientation of Form II crystal lattice in the epitaxially crystallized film. Crystal transformation implies shear parallel to $(100)_{II}$, which brings the $(110)_{I}$ planes in diffracting position.

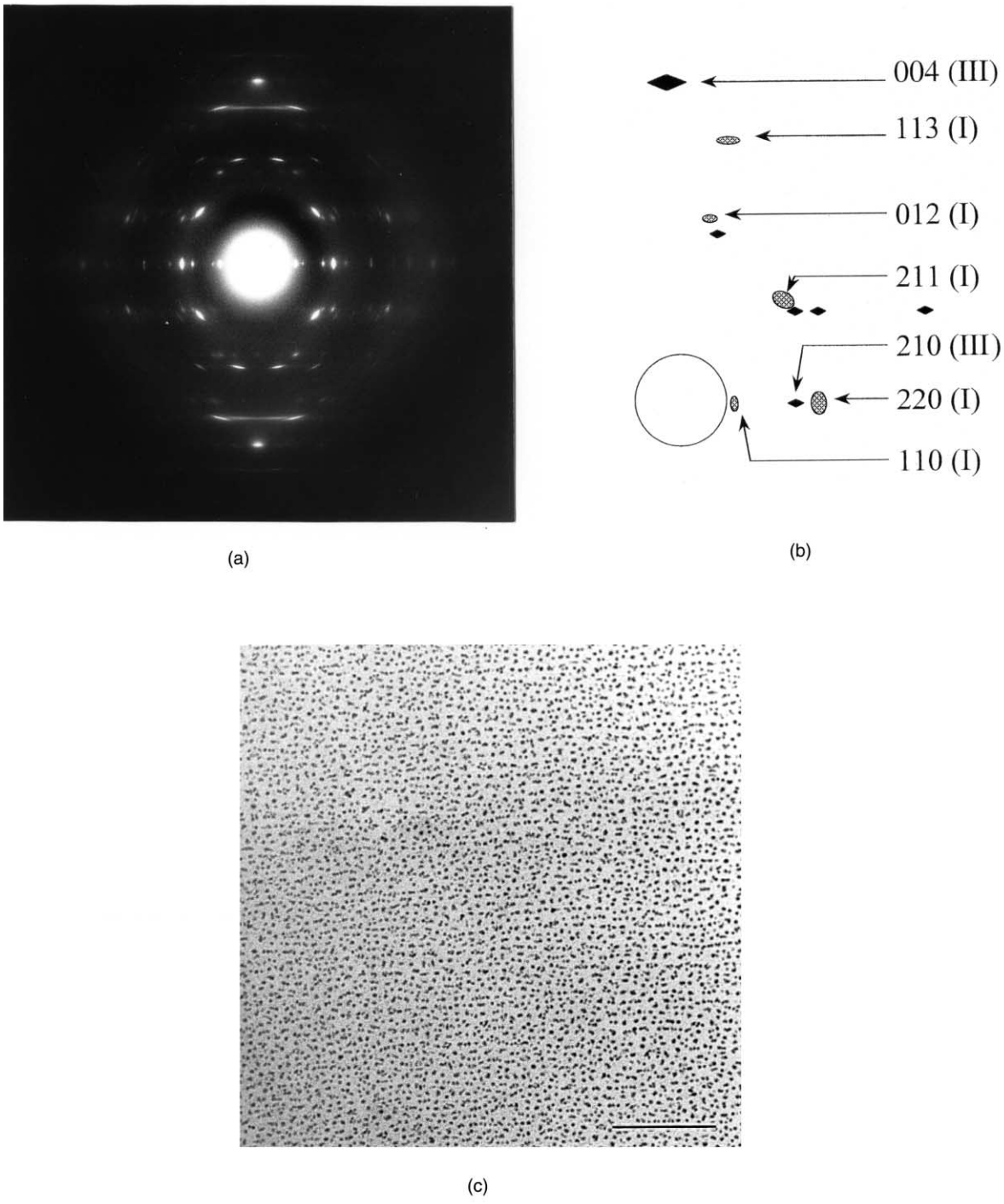

Fig. 4. (a) Electron diffraction pattern of a film of iPBu1 epitaxially crystallized on dicyclohexylterephthalamide (DCHT). (b) Indexing of the pattern in (a). Both Form III and Form II (partially transformed in Form I) are present, with a common chain axis orientation (vertical).(c) Bright field electron micrograph of a composite Form III–Form I (initially Form II) film of iPBu1 epitaxially crystallized on DCHT. The lamellar structure is revealed by gold decoration: the gold droplets gather at the interlamellar zones. However, distinction between lamellae corresponding to the two phases is not possible based on lamellar morphology alone. Scale bar: 200 nm.

patterns analyzed so far lies in the fact *that only one chain orientation is observed for the two forms, which further are colinear*. It is virtually impossible to discriminate Forms II and III by their lamellar morphology. In the diffraction pattern, and as discussed above, Form II is almost converted in Form I: the pattern therefore is a composite of three-fold and four-fold helices with chain axis repeats of 6.5 and 7.4 Å, respectively. The contact plane of Form II (prior to transformation) is again (100) of the tetragonal cell. For Form III, the contact plane is (110). The fact that only one

chain orientation is observed strongly suggests that the epitaxial relationship rests on a lattice matching which involves either the chain axis repeat distance, or the interchain distance. These aspects will be developed later.

3.1.3. Epitaxies of iPBu1 on 3-fluorobenzoic acid: Forms I′, II and III

Nucleation of different crystal forms by specific substrates is commonplace in polymer science. Nucleation of two different phases by the same substrate is not rare, as illustrated above for 4ClBzAc and DCHT. However, in the present investigation, 3-fluorobenzoic acid has been found to induce the three different crystal modifications of iPBu1. Its unit-cell parameters are as follows: $a = 6.81$, $b = 3.81$ Å, $c = 25.90$ Å, $\alpha = \gamma = 90°$, $\beta = 109.2°$, space group $P2_1/c$ [23]. The results are briefly described and summarized, in particular because they provide several examples of epitaxial relationships which help characterize the lamellar morphology of the different phases.

Fig. 5(a) and (b) represent the electron diffraction pattern and bright field (defocused electron diffraction pattern) of a thin film in which both Forms II and I′ coexist (the Form II is already converted to Form I). The pattern is again characterized by four chain orientations, at 24° for Form I′ and 48° for Form I (ex-Form II). The bright field shows very prominently the lamellar orientations of Form II at 48° to each other, which generate clear arrow-head patterns. In the Form I′ lamellar structure it is difficult to recognize the two lamellar orientations. Further, these lamellae abut on lamellae of Form II, and seem to fill the intersticial spaces left by the latter, which indicates that they have grown *after* lamellae of Form II.

As seen in Fig. 5(b), the size of areas made only of Form II or Form I′ is sufficient to isolate the individual phases with a selected area aperture. The resulting patterns are shown in Fig. 5(c) (Form II, partly transformed to Form I) and 5(d) (Form I′). The two patterns display the characteristics expected from the earlier analyses: 48° and 12° angles between the two orientations, 012 reflection common for the two orientations of Form I′, etc.

Fig. 5(e) displays the diffraction pattern of Form III epitaxially crystallized on 3FlBzAc. Note the sharpness of the reflections, and also the fact that the equator is more 'populated' than would be expected for a 'pure' epitaxy, i.e. involving only one contact plane. The additional diffraction spots are however very weak, and the pattern is consistent with a (110) contact plane.

It should be noted that the three above diffraction patterns, and therefore epitaxies, can be observed in any *one* preparation, i.e. the three crystal phases are produced in the same range of crystallization temperatures. We note however that:

- whereas the epitaxies of Forms II and I′ coexist on the same crystals, Form III is produced on its own, on separate 3FlBzAc crystals. This may suggest that (a) another face of the same 3flBzAc crystal form lies in contact with the polymer surface—which is unlikely however in view of the very asymmetric crystal morphology (b) some form of crystal polymorphism of 3FlBzAc is involved in the present versatility. This however could not be checked in the present experiments.
- Crystallization at lower temperatures induces a higher proportion of phase III.
- Whereas the Form II–I transformation is common, no other crystal transformation could be induced by e.g. thermal treatments. In particular, the chiral Form III cannot be converted to either Form II or I, which are racemic.

The epitaxial relationships between 3FlBzAc and the three crystal modifications are discussed in the next section, in relation with the other epitaxies observed in the present investigation.

3.1.4. Structural rules governing the epitaxy of helical polymers

Isotactic poly(1-butene) provides a case example for the analysis of structural rules which govern the epitaxial crystallization of helical polymers. Indeed, to summarize the above observations, we note the following.

Epitaxy of Form I' is completely controlled by the fact that the (110) contact plane in the trigonal cell is made of isochiral helices, which furthermore display a surface topography highly suited for epitaxial interactions. Indeed, the side chains form prominent, very linear rows of methyl and ethyl groups, which are 6.25 Å apart and tilted at 12° to the chain axis normal [8]. The observed epitaxies simply result from the parallel alignment of the rows of side-chains parallel to the substrate chlorine or bromine rows: depending on the helical hand, the chain axis is tilted clockwise or anticlockwise relative to the substrate grating. The two epitaxic orientations share a common 102 reflection: these planes are indeed parallel to the rows of side-chains. The epitaxy clearly involves the *interstrand* distance in the contact plane. Note that the structure of this contact plane is investigated in a later section of this paper by AFM.

Form II is observed in two different patterns:

- Epitaxy of Form II on *4ClBzAc* or *4BrBzAc* generates two orientations, which suggests that, in a way or another, the helical path is also involved. However, the (100) contact plane of Form II contains two antichiral helices: the simple reasoning developed for Form I′ does no longer hold. As analyzed in an earlier paper [3], a dimensional match exists between the two diagonals (≈48° apart) of a substrate lattice made of six cells, three along *b* and two along *a*: the chain axis repeat distance (21.05 Å) is within 5% of this dimension. However, the fact that *three b* repeat units of the substrate are involved suggests that the three-fold helix geometry is also at play. If so, the helical hands and azimuthal settings of the helices in the

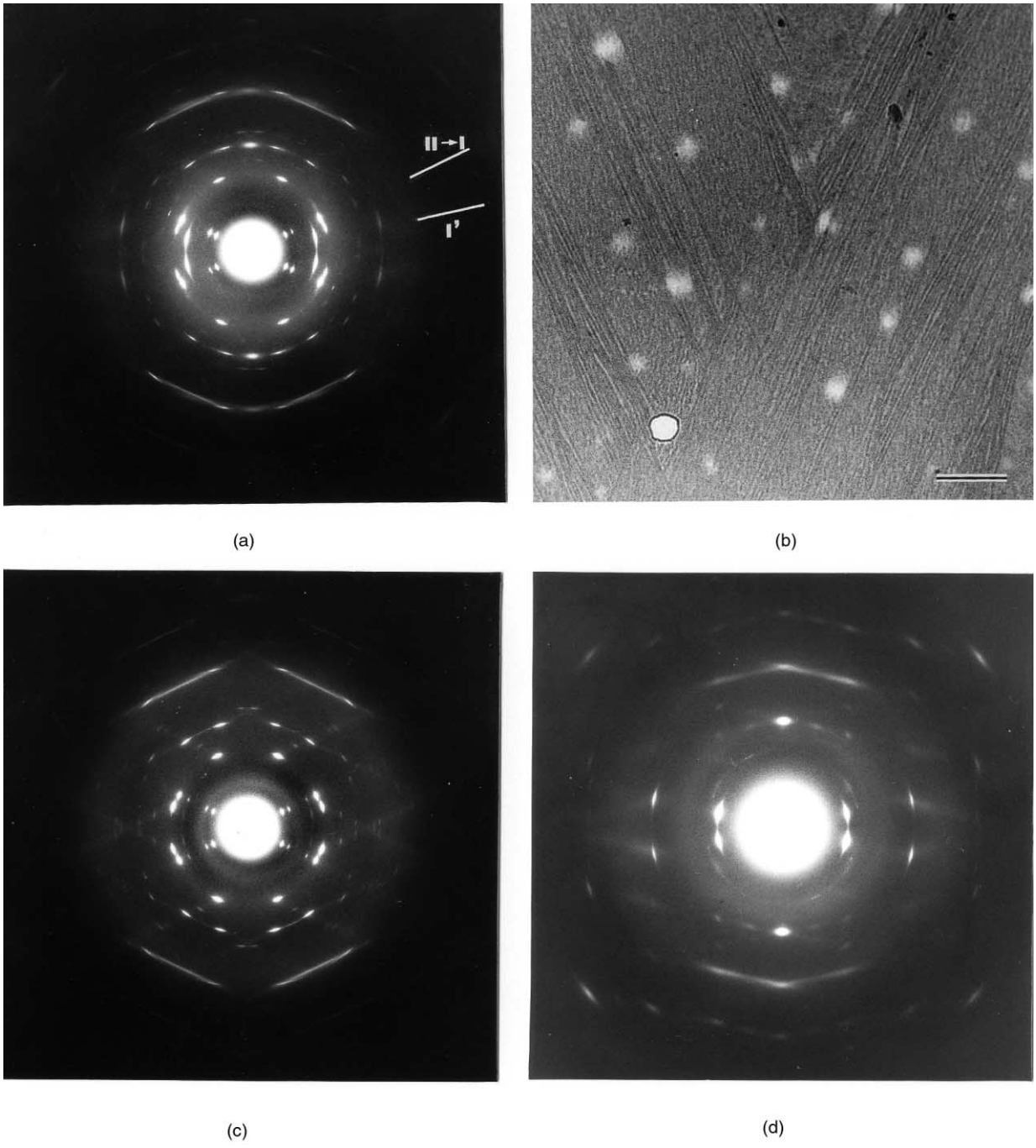

Fig. 5. (a) Electron diffraction pattern of a thin film of iPBu1 epitaxially crystallized on 3-fluorobenzoic acid. The four orientations of the chain axes (two for Form I′, two for Form II, partly transformed into Form I) are similar to Fig. 2(a). (b) Bright field electron micrograph of a film of iPBu1 epitaxially crystallized on 3-fluorobenzoic acid. Lamellae of Form II are more elongated than those of Form I′, which fill the interstitial places, indicating later growth. Scale bar: 1 μm. (c) Selected area electron diffraction pattern of a thin film of iPBu1 as in (b), but by selecting only Form II zones. (d) Selected area electron diffraction pattern of a thin film of iPBu1 as in (b), but by selecting only Form I′ zones. Note the strong 102 reflection on the 'meridian' of this composite pattern, which is common to the two epitaxies of Form I′ at ±12° to the 'meridian'. The pattern shown in part (a) is a combination of (c) and (d). (e) Electron diffraction pattern of a thin film of iPBu1 epitaxially crystallized on 3-fluorobenzoic acid in Form III. Chain axis vertical. (f) The unit-cell of Form III of iPBu1 and the contact plane observed in the epitaxy.

(110) contact plane must be considered in detail, since right and left-handed helices with different settings build up the (100) and (010) faces. Indeed, the azimuthal setting of the chains can highlight or blur the organization of the side-chains in the lateral contact faces: since the azimuthal settings are symmetrical for the two sets of antichiral helices, the surface topography (which is the main concern in epitaxial relationships) of the (100)

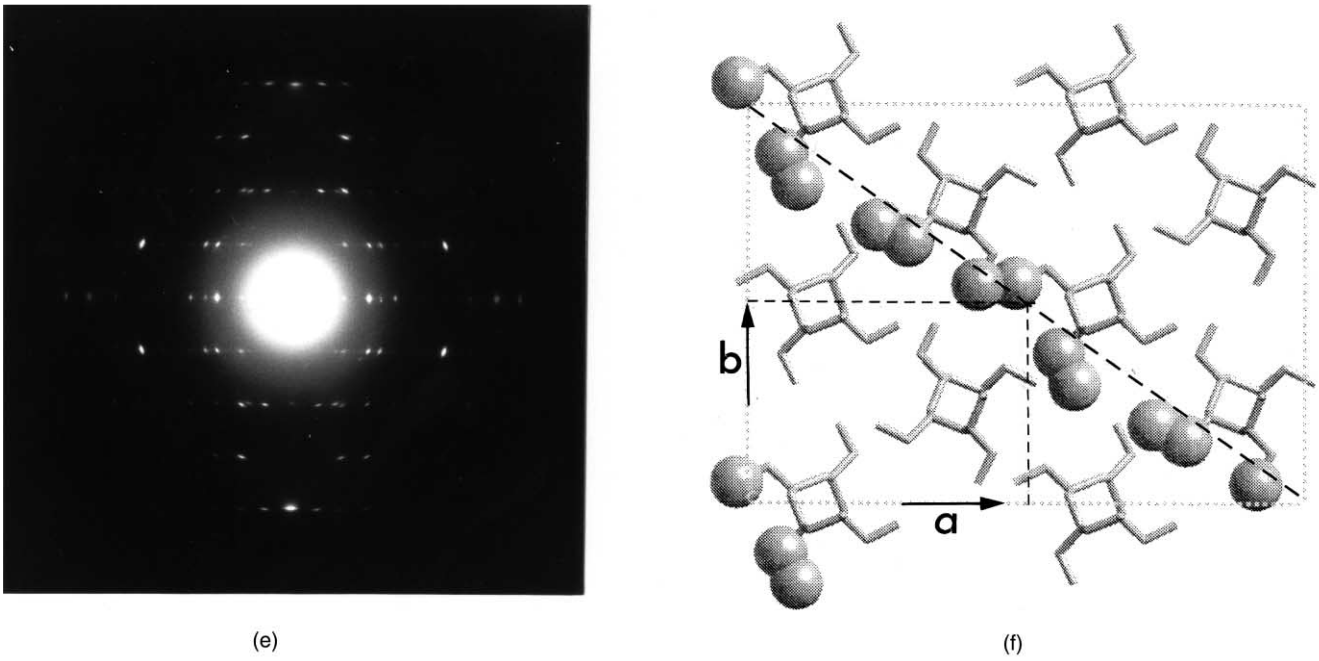

Fig. 5. (*continued*)

contact plane is *antichiral* to the (010) plane. As a result, two symmetrical chain orientations are also generated in spite of the fact that the contact faces are made of antichiral helices. Note that the same reasoning applies for one of the two different epitaxies of Form II on 3FlBzAc, namely that which has two *c* axis orientations.

- The other epitaxy of Form II on *3FlBzAc* and that on *DCHT* generates only one chain orientation, which suggests a lattice matching along, or transverse to the chain axis. In this specific case, *both* matchings seem to be operative, even if the distances involved are large (for the chain axis repeat, this stems from the irrational, 11_3 helix geometry). On 3FlBzAc, *c* of Form II (21.5 Å) matches three *b* repeats (3×6.81 Å $= 20.43$ Å) and laterally, the interchain distance (7.71 Å) matches two *c* repeats (2×3.80 Å).

Form III epitaxy is the most straightforward, although it does not display the anticipated behavior: its crystal structure is chiral, and interactions which highlight this chirality, as for Form I′, could have been expected. These are not observed because the azimuthal setting of the chains differs in the unit-cell, which does not display therefore well organized (110) contact faces (cf. modelization in Fig. 5(f)). In these faces, the most densely populated of Form III, interhelix distances are 7.62 Å (as opposed to 8.88Å in (100)) for a chain axis repeat distance of 7.56 Å. On a geometrical basis, epitaxy appears to rest on a 'conventional' lattice match involving *interchain distances. Two different* matches are however observed: on 3FlBzAc, this is between *nearest* neighbor chains 7.62 Å apart (which match two $c_{3\text{FlBzAc}} = 7.6$ Å) whereas on DCHT it is between *second nearest* neighbor chains 15.2 Å apart (another surprise, but linked with the different azimuthal settings of the chains) and the *triple* of the 5.2 Å substrate periodicity (15.6 Å). This apparently rather unfavorable situation has some logics since the *surface pattern* of the polymer contact face repeats only after every second chain.

In a broader perspective, and beyond the individual analyses of epitaxies, the epitaxial behavior of the three crystal phases of iPBu1 falls in a general pattern illustrated for isotactic polypropylene but which, in the light of the present results, appears applicable to most or all helical polymers. *Three periodicities are accessible in the crystal structures of helical polymers: the interstrand and chain axis repeat distances, and the interchain distances.*

Interchain distances are the essential ingredient in epitaxy of 'linear' polymers, which involves mostly the distance between nearest neighbor stems. In helical polymers however, as seen here for the first time, distances between *second nearest neighbors* may be involved, when the surface topography has this periodicity as a result of different settings of the chains (cf. Form III, possibly also the frustrated structure of βiPP) [11,24] and/or chirality (cf. Form II).

The *interstrand distance* and *chain axis repeat* play similar, although not strictly equivalent roles. When the interstrand distance is highlighted in crystallographic planes made of isochiral helices, it becomes the overwhelming attribute of the epitaxy: this is the basis of Form I′ epitaxy (this contact plane is further analyzed in the next section), and the ingredient which helps determine the helix chirality in the contact plane, due to different chain tilts. For contact planes made of antichiral helices, a similar situation may

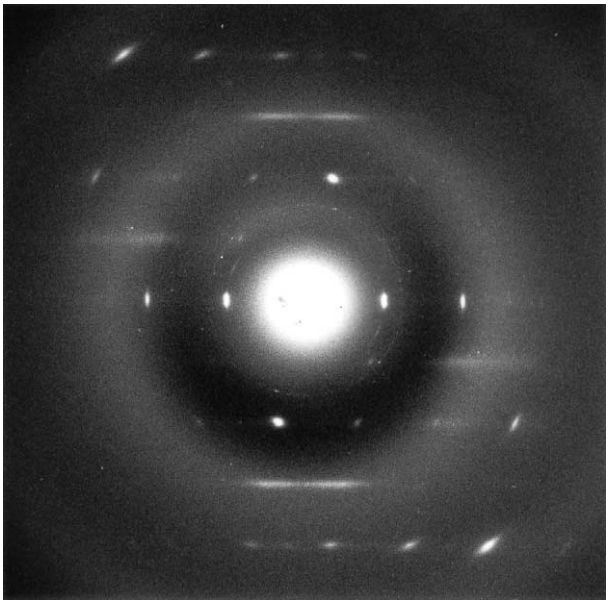

Fig. 6. Electron diffraction pattern of a thin film of iPBu1 epitaxially crystallized in Form I′, which displays only one chain orientation. Chain axis vertical. Note the asymmetry of the pattern relative to the chain axis, indicating a true single crystal character of the epitaxially crystallized film, and the conspicuous presence of streaks, mainly on the first and third layer lines.

exist if one chirality is more 'apparent' in the contact plane due to different azimuthal settings of the chains: it therefore 'guides' the epitaxy and induces the corresponding chain tilt (cf. Form I′, or the (110) contact plane of iPP) [7]. Finally, the helix geometry is also underpinned in epitaxies in which the chain axis repeat is at play. This is most apparent when irrational helices are involved: the (long) repeat distance matches with several substrate unit-cells periodicities. Strikingly however, the global epitaxy corresponds to a *shorter range* one which involves *one helical turn* and one (or at most two) substrate periodicities.

3.2. Up-down helix orientation in Form I′

Epitaxial crystallization of iPBu1 on low molecular weight single crystals generates a crystalline film which has a single crystal texture, in spite of its multi-lamellar morphology. Further, the chain axis lies in the contact plane, which makes it possible to obtain electron diffraction patterns with the layer line organization typical of helical polymers, but in which the structure is seen 'from one side only', and not from all azimuthal orientations as in fiber patterns. Such thin films with well characterized contact planes are exploited in the present section to investigate the issue of up-down orientation of helices in Form I or I′. Two approaches are used: an analysis and modelization of the electron diffraction pattern, and a more local investigation which rests on high resolution AFM of the contact plane.

3.2.1. Electron diffraction data and analysis of the streaks

Electron diffraction patterns of epitaxially crystallized thin films of iPBu1 in its form I′ (as well as that of Form I obtained by solid–solid transformation of Form II) display both sharp reflections and streaks (cf. Fig. 6, which is similar to Fig. 5(d), but from an area of the film in which one chain direction is predominant). The underlying structural disorder rests on the possibility to substitute at any one helix site an up-pointing helix by a down-pointing one. As indicated by Natta et al. [8] in the very first structure derivation of Form I, such a substitution is structurally very likely, since anticline helices have very similar external shapes: anticline isochiral helices are nearly isosteric (cf. Fig. 7(a) and (c), which correspond to classical figures of Natta and Corradini's paper). However, the substitution does restore the atomic positions for the outermost methyl groups of the side-chains only: all other atoms of the chain have slightly different fractional coordinates (Fig. 7(a) and right hand side of 7(c)). These slight differences are at the root of the streaking observed in the diffraction pattern.

Similar streaks and features are frequent in polymer crystallography. Best known examples deal with the up-down substitution in isotactic polypropylene in its α phase (αiPP), which exists in two so-called 'limiting ordered crystal phases': α_1, corresponding to statistical occupancy of up- and down-helices at each chain site, and an α_2 crystal phase in which *bi*layers made of all isocline helices alternate with similar bilayers in which the helices are anticline to the first one. The two structures have different space groups: $C2c$ and $P2_1/c$, and differ therefore by the presence or absence of specific reflections, most visible on the first layer line of the fiber pattern [25].

The diffraction patterns displayed in Fig. 6 show slightly different features, in that the streaks are definitely located on specific layer lines, most prominently on the *odd* ones: first and third. Moreover, the streaks on the first layer line are *not* symmetrical with respect to the chain axis direction. Note that this feature can only be observed because the epitaxy selects one specific helical hand in the contact plane and generates a true *single crystal*—although multilamellar—structure.

Modelization of the structural disorder is performed with the help of the 'Diffraction faulted' module of the Cerius 2 program [14]. Technically, some constraints of the program make it necessary to redefine the unit-cell geometry and to relabel the crystal axes: streaks are always calculated along the reciprocal c^* axis. To conform to the program limitations, a monoclinic unit-cell made of four individual chains (two of each layer of a bilayer) is generated (Fig. 7(b)), which is packed with the appropriate shifts to recreate the bilayer structure in the (110) plane of the trigonal unit-cell. Note that this monoclinic 'unit-cell', although unusual, is yet another way to describe the trigonal crystal structure of iPBu1, which can also be reduced to a smaller, triclinic unit-cell made of the two center chains in Fig. 7(a). The full pattern is split in its 'positive' and 'negative' parts, which

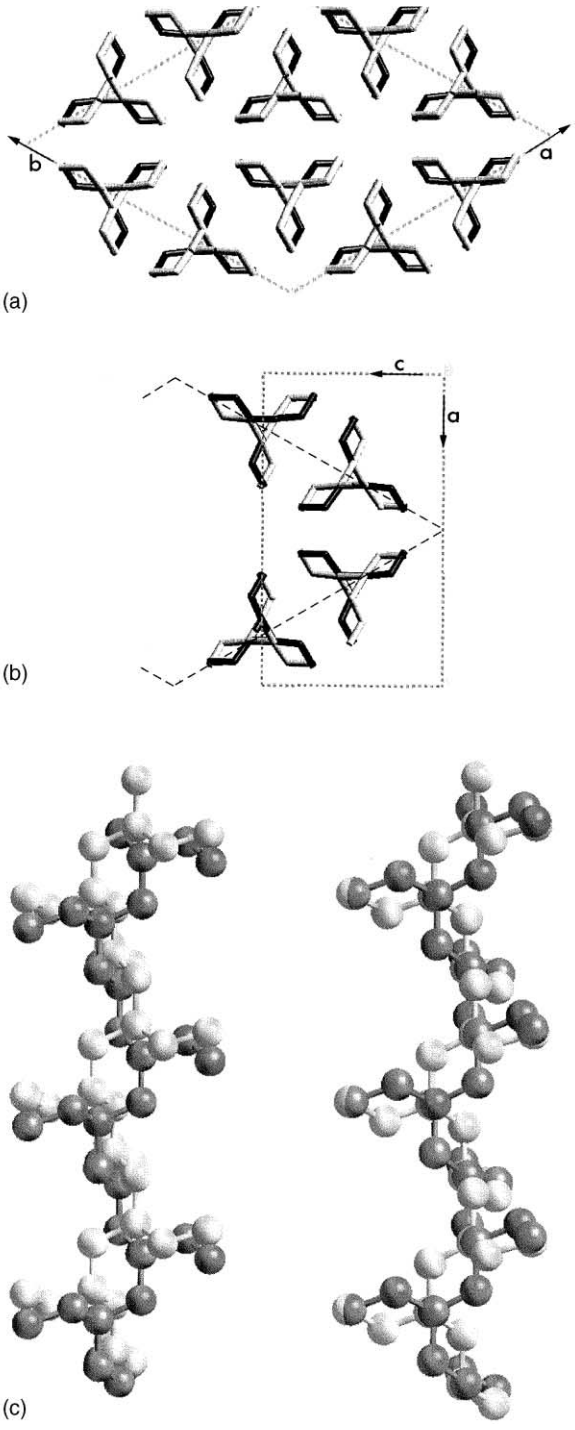

Fig. 7. (a) The crystal structure (seen in chain axis projection) of Form I′. The trigonal unit-cell contains six three fold helices, organized in layers of isochiral helices, alternating layers being antichiral. In the R-3c space group illustrated here, statistical occupancy at each chain site by an up-pointing and a down-pointing chain (shown in light and dark grey) is assumed. (b) The simpler unit-cell used in the modelization of the disorder, with the choice of axes imposed by the program. Various combinations of up- and down-pointing helices are used. (c) The substitution of up and down helices at a given site, as 'seen' by the electron beam in Fig. 6. On the right: location of outside methyl groups maintained fixed. On the left: additional *c* axis shift associated with the substitution, as suggested by the present study.

can also be thought of as the compounding of two equivalent (say positive) 'half' patterns of the same stack of layers seen from opposite sides. As indicated, this type of information is *only* accessible through electron diffraction of a 'single crystal type' thin film as produced by epitaxy, but is lost in a fiber pattern.

Modelization performed by assuming that the location of the outside methyl groups is maintained unchanged in up-and down-pointing helices and assuming strict egality of up- and down-pointing helices does not yield any streaks, as would be expected: we are dealing with a true R-3c symmetry. Introduction of some disorder in up and down probabilities does yield the blend of streaks and sharp reflections observed in the fiber pattern. However, some intensity inversions remain, in particular a calculated excessive strength of reflections on the fourth layer line as compared to e.g. the second layer line. This suggests that some other disorder is also at play, and most probably shifts along the chain axis. A reasonable fit with the experimental data is found for $\approx \pm 0.5$ Å shifts (Fig. 7(c), left hand side). The resulting calculated intensity profiles on the equator and the four first layer lines are represented in Fig. 8 (note that the intensity scales have been adjusted for each layer line). This diagram displays all the characteristics of the actual diffraction pattern, even if some minor discrepancies remain. The diffraction peaks and streaks are well reproduced both in terms of extent and location (which implies asymmetry) on the equator, second and fourth layer lines (for the diffraction peaks) and on the critical first and third layers for the streaks. Note that this analysis applies also to the structure of Form I, obtained by solid–solid transformation of Form II: the diffraction patterns of Form I display also streaks—which however are symmetric, since epitaxial crystallization of Form II is not 'stem chirality selective' in the contact plane. Their analysis is however complicated by the fact that different azimuthal orientations of the unit-cell coexist as a result of the transformation mechanism described in Fig. 3: their modelling has not therefore been attempted.

The modelling of the diffraction pattern and the very simple hypotheses on the structural disorder just described (chain inversion associated with a slight *c* axis shift) are fully consistent with the structure derivation of Form I or I′ by Natta et al., and support their conclusions about the structural disorder of iPBu1 [8]. The present analysis leads to a slight relaxation of the idealized structural disorder described so far, which assumed, for simplicity, identical location of the ouside methyl groups in the up- and down-pointing chains. Note however that the *c* axis shift introduced in the model stems from a discrepancy in intensities of diffraction spots rather than streaks, and is apparent also from a simple analysis of the calculated intensities assuming R-3c symmetry. This (slight) modification of the model is not actually a direct outcome of the modelling of the streaks performed in the present work. Finally, it should be mentioned that the present analysis does not use *quantitative*

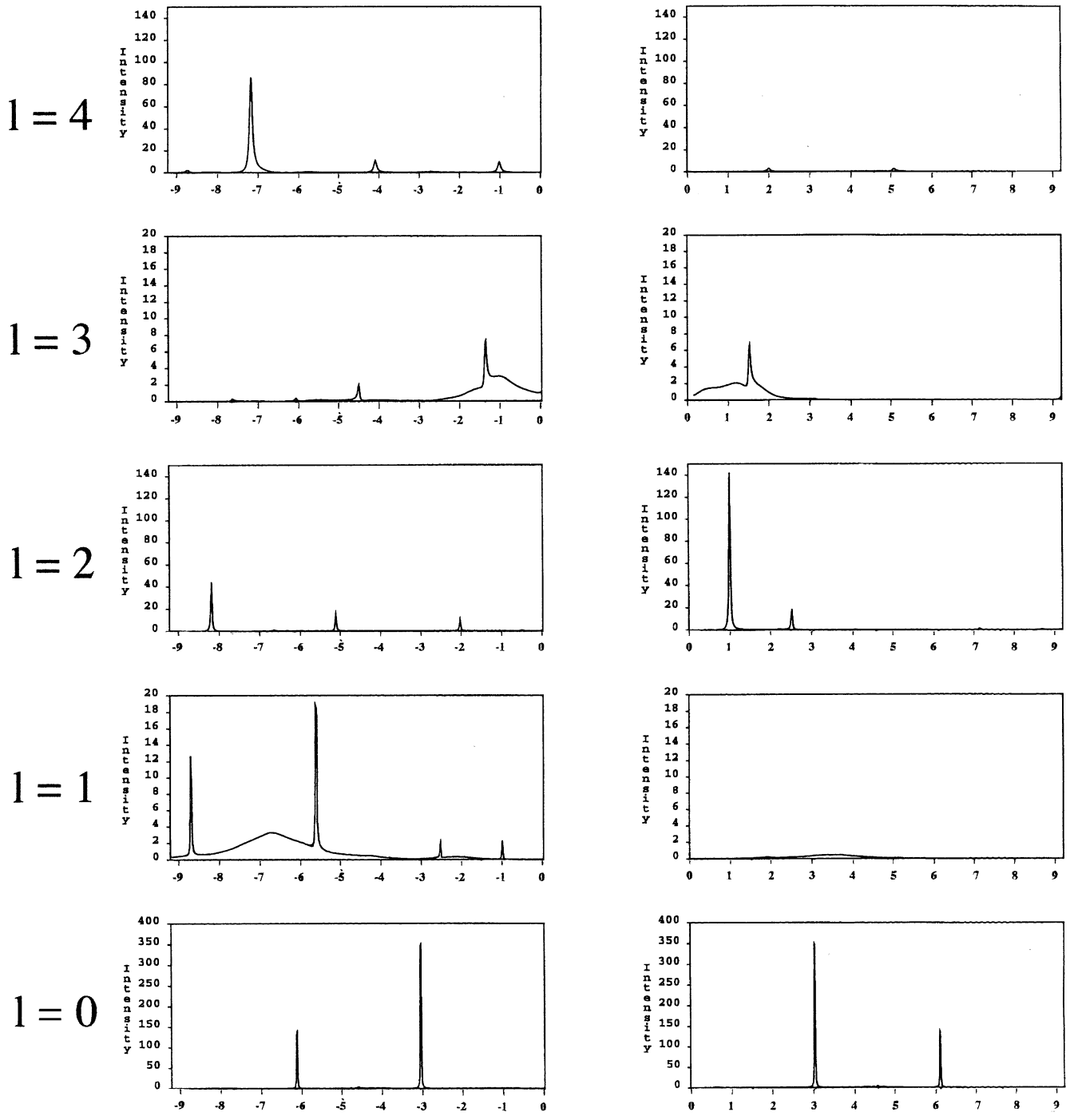

Fig. 8. Intensity profiles for layer lines 0–4 computed for a crystal structure of Form I′ with random positioning of up and down helices. The computed profiles illustrate the major features of the diffraction pattern in Fig. 6: strong reflections on even layer lines, weaker reflections and streaks on the odd layer lines (highly asymmetric and spread on the first, symmetric on the third layer). The intensity scales are expanded for the odd layers. Reduction of the −704 reflection intensity achieved through a shift of the chains by ≈±0.5 Å along the chain axis, which seems to be a genuine feature of the statistical structure (cf. Fig. 7(c)).

intensity diffraction data. It relies mostly on a visual comparison of intensities of the weak spots in the diffraction pattern and the streaks. Clearly (as also advocated by one referee of this paper), a more quantitative analysis is called for. This will be the subject of future work.

3.2.2. Up-down helix orientation in Form I′: AFM experiments

The above analysis is a *global* evaluation of the up-down disorder of iPBu1, form I′. However, the contact plane of Form I′ offers—potentially—a possibility to determine the

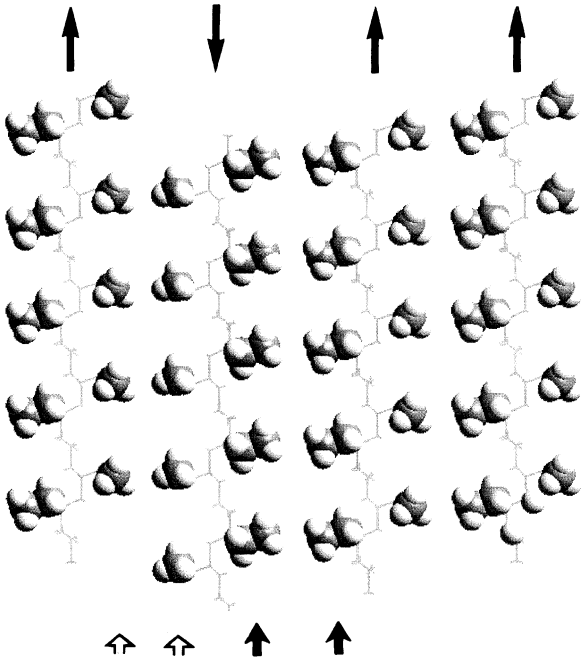

Fig. 9. A possible means to identify chain orientation in the (110) contact plane of iPBu1 Form I′. Four chains are shown, which expose either ethyl and methyl groups on the sides of the helix axis. One chain is anticline to the three others (top arrows). As a result, the regular alternation of ethyl and methyl rows is perturbed, with two neighbor rows of ethyl groups (bold arrows, bottom) or two rows of methyl goups (open arrows). Chain axes *must* be located *outside* of these double rows.

true helix orientation of *individual* helices. While this technical feast has not been achieved in the present investigation, the problematics and the technical limitations encountered are worth being presented, as they may be revived when AFM performance is improved.

At a molecular (or more precisely *stem*) level, the structural manifestation of up-down disorder in the contact face is the replacement of an ethyl group by a methyl group. More exactly, the $C(H_2)$–$C(H_3)$ bond of any one helix is located in the (110) plane of the unit-cell. The next (or the previous) ethyl side chain has its $C(H_2)$–$C(H_3)$ bond oriented at 120° to the initial one (located in the (−210) or (2−10) plane), but its end methyl group is located in the *same* (110) plane as the neighbor ethyl group along the chain (Fig. 7(a)). Moreover, the exposed methyl group and ethyl groups are located on opposite sides of the chain axis in the (110) plane. When the helix sense is reversed (second chain from the left), the positions of the ethyl groups and methyl groups are reversed relative to the chain axis (Fig. 9). *The sequence of exposed, parallel rows of ethyl and/or methyl groups depends on the sequence of relative helix senses*: alternating methyl and ethyl rows indicate parallel (syncline) helices; two neighbor methyl (or ethyl) rows indicate antiparallel (anticline) helices. The helix axes positions, located below the surface, can be deduced from the pattern of ethyl and methyl rows in the contact face. The chain axis is always located between neighbor ethyl and methyl rows. In areas with parallel helices (right side of Fig. 9) this leaves an ambiguity about the exact position of the chain axis, which is relieved when an anticline helix is present. Indeed, anticlinicity is manifested by at least two neighbor rows of identical side chains (say methyls or ethyls). These cannot belong to the same helix, which positions the helix axes *outside* the double rows of identical side-chains. The position of all other helix axes in the layer is then unambiguously defined, since the inter-helix distance is known (≈10 Å).

The above analysis sets the stage for the technical challenge: if AFM can discriminate ethyl and methyl groups in the (110) contact plane, the up or down orientation of every stem can be defined. This goes beyond the resolution limits reached so far in AFM of crystalline polymers and more specifically of epitaxially crystallized polymers investigated in earlier studies. Let us recall that methyl group resolution was reached when investigating the contact plane of isotactic polypropylene in both α [9,10] and β phase [11]. For epitaxially crystallized syndiotactic polypropylene, the best images have a resolution better than the methyl group radius (the Fourier transform displays a diffraction spot at 1.9 $Å^{-1}$). This high level of resolution is probably linked with a number of favorable features—which are also found in the present films of iPBu1: (a) the surface is molecularly smooth, since it corresponds to the imprint of the low molecular weight substrate crystal (b) the sub-molecular features (e.g. methyl groups) are arranged in a crystallographic pattern: the experimental images can therefore be confronted with the images anticipated from the crystal structure.

In the present case, the ethyl and one methyl group are located in the (110) contact plane of Form I′. The AFM challenge is therefore to distinguish a methyl group (a sphere of diameter 4 Å) from an ethyl group (a more elongated ellipsoïd 4 Å wide by 5.5 Å long; the added length corresponds to the C–C bond). This appears undoubtedly difficult, but one may take advantage of the possibility to image *whole rows* of these groups aligned along the *c* axis of each helical stem.

Our approach to analyze the surface structure of epitaxially crystallized iPBu1 films is similar to that used for the various investigations on tactic polypropylenes [9–12]. The thin film is freed from the low molecular weight substrate material by selective dissolution, the (now exposed) areas of interest are first selected under the optical microscope by taking advantage of the imprint left in the polymer film by the substrate crystal. AFM examination is performed in a liquid environment. The best image obtained is shown in Fig. 10. It displays a number of characteristic features of the crystal structure and more precisely the contact plane of Form I′: it shows a clear chain axis direction, with a repeat distance of 6.5 Å. It also shows parallel rows 6.3 Å apart, which are tilted by 12° relative to the chain axis. These correspond to the rows of ethyl and methyl groups mentioned earlier and which are located in the (110)

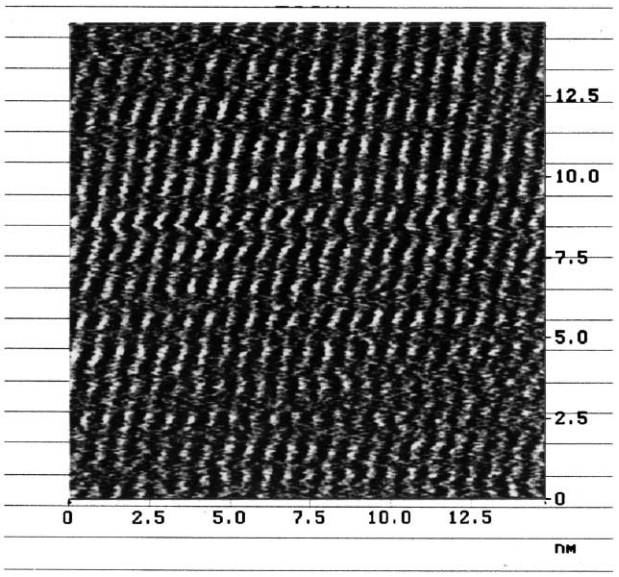

Fig. 10. Atomic Force Microscope image of the (110) contact plane of iPBu1 epitaxially crystallized on 4-chlorobenzoic acid. The chain axis is horizontal: the linear grating added to the outside of the image indicates the interchain distance (but *not* the position of the chain axes, which cannot be deduced from this image). The helices imaged are left-handed: *oblique* rows of ethyl *and* methyl are clearly visible, but *not* the rows of ethyl *or* methyl groups *parallel* to the chain axes, which would help establish the position of the chain axes and the relative chain sense.

crystallographic plane. Since the chain axis orientation and the tilt of the helical path are both visible, the helix hand in the exposed contact face can be determined directly: in Fig. 10, the helices are left handed. The resolution falls however slightly short of allowing recognition of the individual ethyl and the methyl groups, or even of *whole rows* of these groups parallel to *c*. In order to help 'read' the image shown in Fig. 10, it is surrounded with a grating representing the orientation of the chain axes, with the characteristic $\approx$10 Å interchain distance.

The origin of this resolution failure is difficult to analyze. Of course, it may be linked with an instrumental deficiency or a mismanipulation: the technique is indeed very 'touchy' when dealing with this level of resolution. If this is the main cause of the present failure, it will be of interest to reconsider this problem when better instruments or tips are available. Other causes may however be invoked, and we will concentrate on one of them, namely the possible 'blur' introduced in the AFM image by movements of the side chain methyl groups.

Molecular movements in the contact plane do not affect the main chains, which are solidly attached to the substrate surface along their entire length. Our previous experience with iPP and sPP contact surfaces indicates that there is little or no 'surface reconstruction', as for example reorientation of chains on their axes. Movements may however affect *sub-groups*. In particular, the end methyl group of the ethyl group 'exposed' in the contact plane can rotate, or at least 'flip' since this movement is no longer constrained by the crystallographic environment. The rotational angle of the C(H)–C(H_2) bond is involved, which is at an angle to the (110) plane: at its 'peak' position outside the (110) plane, the methyl group is much closer to the chain axis, (in projection, i.e. on a two dimensional image as produced by AFM), and only slightly higher above the 'background' (110) plane. The difference between ethyl group and methyl group would be all the more difficult to capture by AFM, both in lateral position and height.

Finally, it is worth comparing the present AFM experiments with recently published results on a somewhat similar material by Winkel and Miles [26]. These authors use ultra-thin films of iPBu1 produced by the Petermann-Gohil [27] draw technique, which have a *fiber* type structure: only the *c* axis orientation is determined (parallel to the draw direction), while the *a* and *b* axes orientations are not controlled. AFM images help identify the crystal structure (in aged films initially in Form II, this is Form I) and the nature of the exposed planes by comparing the surface topography and periodicities with the Connally surfaces of various low index crystallographic planes—apparently a Form I structure with parallel helices (R3c symmetry); the issue of chain orientation is not considered. Winkel and Miles identify the Form I chain axis periodicity and, on one investigated film surface, identify (1–10), (100) and (0–10) exposed planes [26]. The present approach, which combines epitaxial crystallization and AFM, is comparatively more 'guided' by the polymer crystallography and epitaxial interactions: the crystal phases and exposed faces *are known*, and can be controlled. The images of Winkel and Miles, and notably their Figure 4(a), are of course relevant to the present problematic of up-down chain orientation. However, and even though a 2 Å resolution is mentioned, our analysis of the published images does not allow recognition of the relative helix orientations.

To summarize this section, epitaxial crystallization of iPBu1 in its form I′ provides 'single crystal type' diffraction data which can be used to get further insight in the structural disorder of this phase. In agreement with the earliest analyses of the crystal structure, the streaks of the pattern result from randomness in the up-down orientation of the chains. The relative intensity of streaks and diffraction spots suggests that substitution of up- and down-pointing chains introduces an additional *c* axis shift of the whole chain, which we evaluate to be about $\pm$0.5 Å.

The (110) contact face of iPBu1 provides a potential material to investigate by AFM the up- or down-orientation of every helical stem in the contact plane—a technical challenge and a further frontier for the local scale analysis of polymer crystal structures. The conceptual and experimental approaches used in this investigation appear valid. Recognition of helix sense of three-fold helical structures packed in the very favorable trigonal unit-cell with R-3c symmetry with exposed (110) contact planes rests on the differentiation between side-chains topographies on the two sides of the helix axis in the contact plane. Our attempts at

imaging the helix orientations of iPBu1 have fallen only slightly short of achieving this further insight, possibly as a result of lack of resolution, but possibly also because the topographical (structural) difference between the two 'sides' of the helix is insufficient. Polymers with bulkier side chains (which would help overcome the present problems of resolution) and/or which display more important structural differences (e.g. more important tilt of the side chains, as e.g. in isotactic polystyrene) may be more appropriate for this type of investigation.

4. Conclusion

Epitaxial crystallization of isotactic poly(1-butene) and generation of its different crystal modifications has been further explored by investigating the impact of various low molecular weight nucleating agents which have been found to be efficient for other polymers, and notably for polyolefins. The new results confirm that all three crystal structures can be induced by appropriate nucleation additives. In particular, we have observed that one substrate—3-fluorobenzoic acid—is able to induce all three crystal modifications of iPBu1 depending on crystallization temperature. Such a versatility is only seldom encountered in epitaxial crystallization of polymers.

Epitaxially crystallization of polymers generates thin films with uniplanar biaxial or even single crystal unit-cell orientations. By taking advantage of such materials, the issue of relative helix orientation has been reconsidered for Form I′, both by analysis of the diffraction pattern and by AFM. The global analysis confirms the existence of a statistical up-down orientation of helices, which is accompanied by slight shifts of the whole helix along the *c* axis direction. Determination of the orientation of *individual* helical stems has been attempted by AFM imaging. This endeavor rests on the fact that in the (110) contact plane, anticline three-fold helices differ by the location of exposed side-chains. Whereas our AFM images reveal the helix chirality, their resolution is insufficient to yield the more detailed information needed to characterize the helix sense. The conceptual and experimental approaches remain however valid, and should be applied in the near future to polymers with bulkier side chains.

References

[1] Luciani L, Seppälä J, Löfgren B. Prog Polym Sci 1988;13:37.
[2] Wittmann JC, Lotz B. Prog Polym Sci 1990;15:909.
[3] Kopp S, Wittmann JC, Lotz B. Polymer 1994;35:908.
[4] Kopp S, Wittmann JC, Lotz B. Polymer 1994;35:916.
[5] Dorset DL, McCourt MP, Kopp S, Wittmann JC, Lotz B. Acta Cryst 1994;B50:201.
[6] Mathieu C, Thierry A, Wittmann JC, Lotz B. Polymer 2000;41:7241.
[7] Yan S, Katzenberg F, Petermann J, Yang D, Shen Y, Straupé C, Wittmann JC, Lotz B. Polymer 2000;41:2613.
[8] Natta G, Corradini P, Bassi IW. Nuovo Cimento Suppl 1960;15:52.
[9] Stocker W, Magonov SN, Cantow HJ, Wittmann JC, Lotz B. Macromolecules 1993;26:5915; Corrections: ibid, 1994;27:6690.
[10] Stocker W, S, J, JC, W, Graff S, Lang J, Wittmann JC, Lotz B. Macromolecules 1994;27:6677.
[11] Stocker W, Schumacher M, Graff S, Thierry A, Wittmann JC, Lotz B. Macromolecules 1998;31:807.
[12] Stocker W, Schumacher M, Graff S, Lang J, Wittmann JC, Lovinger AJ, Lotz B. Macromolecules 1994;27:6948–55.
[13] New Japan Chemical Co, Ltd, European Patent EP 93101000.3, Japanese Patents JP 34088/92, JP 135892/92, JP 283689/92, JP 324807/92, 1992.
[14] Cerius^2 4.0 Program manual, Molecular Simulations Inc., Waltham, USA and Cambridge, UK, 1997.
[15] Treacy MMJ, Newsam JM, Deem MW. Proc R Soc Lond A 1991; 433:499.
[16] Miller RS, Paul IC, Curtin PY. J Am Chem Soc 1974;96:6334.
[17] Ohkura K, Kashino S, Haisa M. Bull Chem Soc Japan 1972;45:2651.
[18] Holland VF, Miller RLJ. Appl Phys 1964;35:3241.
[19] Fujiwara Y. Polymer Bull. 1985;13:253.
[20] Kopp S, Wittmann JC, Lotz BJ. Mater. Sci. 1994;29:6159.
[21] Lotz B, Mathieu C, Thierry A, Lovinger AJ, De Rosa C, Ruiz de Ballesteros O, Auriemma F. Macromolecules 1998;31:9253.
[22] Mathieu C, Thierry A, Wittmann JC, Lotz B. Submitted.
[23] Toga T, Yamamoto N, Osaki K. Acta Crystallogr. Sect. C 1985;41: 153.
[24] Dorset DL, McCourt MP, Kopp S, Schumacher M, Okihara T, Lotz B. Polymer 1998;39:6331.
[25] Natta G, Corradini P. Nuovo Cimento Suppl 1960;15:40.
[26] Winkel AK, Miles MJ. Polymer 2000;41:2313.
[27] Petermann J, Gohil RMJ. Mat Sci 1979;14:2260.